3D primary estimation by sparse inversion using the focal domain parameterization

G. A. Lopez, D. J. Verschuur, Delft University of Technology*

SUMMARY

Recently, a new approach to multiple removal has been introduced: estimation of primaries by sparse inversion (EPSI). Although based on the same relationship between primaries and multiples as surface-related multiple elimination (SRME), it involves quite a different process: instead of prediction and subtraction of multiples, in EPSI the unknown primaries are the parameters of a large-scale inversion process. Based on a sparseness constraint, primaries are estimated in such a way that - together with their corresponding surface multiples - they explain the input data. In this paper a new algorithm is proposed to extend the EPSI process to the full 3D case, in which data reconstruction and primary estimation are combined, based on parameterization of the primaries in the so-called focal domain. This algorithm will allow reconstruction of large data gaps and yields reliable primaries. Results of this algorithm for a simple 3D example are shown.

INTRODUCTION

In surface-related multiple elimination (SRME) (Berkhout, 1982; Verschuur et al., 1992; Berkhout and Verschuur, 1997; Weglein et al., 1997; Biersteker, 2001) the multiples can be predicted without any prior knowledge of the subsurface. All of the required information is embedded in the seismic data, because of the strict relationship between primaries and multiples.

However, the 2D implementation falls short with the increased emphasis on high-fold 3D data with wide-azimuth geometries. Therefore, a great effort was put in the early 2000's to make the SRME method 3D (Biersteker, 2001; Lin et al., 2004; Moore and Bisley, 2005; van Dedem and Verschuur, 2005; van Borselen et al., 2005; Baumstein et al., 2005). Nowadays, 3D SRME is not necessary free of approximations, as today's 3D acquisition geometries do not provide all the measurements required for a full 3D SRME. Therefore, current implementations of 3D SRME require fast and cheap on-the-fly data interpolation (Dragoset et al., 2008; Aaron et al., 2008; Dragoset et al., 2010; Smith et al., 2011).

In addition to the implementation of 3D SRME, recently a new approach to multiple removal was developed by van Groenestijn and Verschuur (2009a): estimation of primaries by sparse inversion (EPSI). Several data examples for EPSI were discussed in Savels et al. (2011). The main difference with SRME is that in EPSI the two-stage processing method, being prediction and adaptive subtraction, is replaced by a full waveform inversion process. The primary reflection events are the unknowns in this algorithm and are parameterized in a suitable way. In van Groenestijn and Verschuur (2009a) the used parameterization consists of band-limited spikes and an effective source wavelet. Baardman et al. (2010) discussed a refinement, where the wavelet was made time-variant in order to include the change of the observed seismic wavelet in case of complex propagation effects (fine layering, dispersion) and absorption. Lin and Herrmann (2010, 2011) showed that the primary impulse response can also be defined in the curvelet domain, rendering a more efficient parameterization. The L1 implementation of EPSI was used by Doulgeris et al. (2012) to achieve joint multiple removal and deblending.

A major advantage of EPSI is that the adaptive subtraction, involved in SRME, is avoided. Instead, in EPSI the full input data is explained, being the sum of the estimated primaries and their associated surface multiples. The new objective function - the difference between the input data and the estimated primaries plus their multiples - will truly go to zero. Furthermore, missing data can be estimated together with the primaries, such that the method has great virtue in the situation of shallow water (van Groenestijn and Verschuur, 2009b).

Due to the great promise of the EPSI algorithm in 2D cases, a 3D EPSI algorithm is envisaged. For this, however, new challenges must be faced. The most important one is related to coarse sampling: in most of the current 3D acquisition geometries the required data volume needed to achieve proper multiple estimation is heavily under-sampled. Typically one direction (e.g. the in-line direction) has a much denser sampling than the other direction (the cross-line direction). All the acquisition holes present in the data volume must be filled with physical information for correct multiple prediction. One option is to use some simple interpolation method as a preprocessing step to fill all the missing traces, as commonly done with 3D SRME (Dragoset et al., 2010). However this step can lead to strong artifacts and wrongly predicted multiples if the amount of missing data is large compared with the required data volume, or if the multiple generating reflectors are shallow, as normally the interpolation quality reduces notably when the reflectors are approaching the surface.

In order to accurately predict multiples in coarse 3D acquisition geometries, a new parameterization must be adopted to allow EPSI to effectively reconstruct data over large gaps. We will use the bi-focal transform (Kutscha et al., 2010) for sparsely representing the earth's primary impulse responses. The bi-focal transform is a generalization of the earlier introduced focal transform (Berkhout and Verschuur, 2006) and aims at focusing primary reflections into localized spikes. In the focal domain all the information coming from the different earth layers is mapped into localized events that correspond to the reflectivity of each layer. Once these reflectivity events are obtained, they can be used to explain all data, given the propagation operators to the most important layers. In this way missing data and source signatures can be effectively reconstructed, allowing precise multiple predictions. Note the reconstructed data will remain physically correct (both in amplitude and kinematics) independently of the depth of the water layer.

In the following we will give the theoretical background along

DOI http://dx.doi.org/10.1190/segam2013-1129.1

with some examples to explain the new EPSI algorithm.

THEORY

For the EPSI algorithm we first start with the basic expression for the upgoing wavefield $\mathbf{P}$ at the surface (Berkhout, 1982; Verschuur and Berkhout, 1997):

$$\mathbf{P} = \mathbf{X}_0\mathbf{S} + \mathbf{X}_0\mathbf{R}^{\cap}\mathbf{P}, \tag{1}$$

where $\mathbf{X}_0$ contains the impulse responses of the earth without a reflection surface, $\mathbf{S}$ is the source matrix and $\mathbf{R}^{\cap}$ is the reflection operator at the surface. In practice the source matrix can be taken diagonal if all the shots have the same source signature $\mathbf{S}(\omega) \approx S(\omega)\mathbf{I}$, also the reflection operator at the surface can be taken as $\mathbf{R}^{\cap} \approx R^{\cap}\mathbf{I} \approx -\mathbf{I}$ for the marine case (we will leave it here as $R^{\cap}$ to avoid loosing generality). Furthermore, $\mathbf{X}_0$ can be described by (Berkhout, 1982):

$$\mathbf{X}_0 = \sum_{m=0}^{\infty} \mathbf{W}_m^T \mathbf{R}_m^{\cup} \mathbf{W}_m, \tag{2}$$

were the $\mathbf{W}_m$ describes wavefield propagation between the surface and depth level z_m. The above equation describes the full impulse response of the earth in terms of elastic reflections at all depth levels, where reflection matrices $\mathbf{R}_m^{\cup}$ contain the reflection properties at depth level z_m (Berkhout, 1982; de Briun et al., 1992). This forward model was derived to describe migration algorithms. Note that all matrices can be interpreted in a full 3D sense, as shown by Kinneging et al. (1989).

For the purpose of parameterizing $\mathbf{X}_0$, the infinite sum can be relaxed if we mentally divide our depth range in effective *focal regions*, bounded by their respective *focal boundaries*. A typical strategy is to divide the subsurface in different parts such that the boundaries between the focal regions correspond to the strongest reflecting boundaries. In this way we account for the major part of the reflected energy via the focal boundaries, while leaving the low impedance reflectors information inside the focal regions. This can be done without loosing generality if we allow the reflectivity matrices to contain information beyond their reflection ($t = 0$) time. This allows a finite summation in equation 2, which can be written as:

$$\hat{\mathbf{X}}_0 = \sum_{m=1}^{M} \hat{\mathbf{W}}_m^T \hat{\mathbf{R}}_m^{\cup} \hat{\mathbf{W}}_m, \tag{3}$$

where M is the number of focal regions, and the 'hatted' operators are now the estimates of the corresponding quantities, given that the exact variables may be unknown. In equation 3 the detailed structure of every focal region will now be encrypted in the frequency content of the effective reflectivity matrix $\mathbf{R}_m^{\cup}$ for the focal region into consideration; in this way no information is lost.

Once the strongest reflectors are recognized (focal boundaries) the EPSI inversion procedure can start. The inversion aims to estimate: (1) The effective reflectivity information in all the M focal regions $\hat{\mathbf{R}}_m^{\cup}$, $m \in [1, M]$, (2) the source wavelet $S(\omega)$, and (3) the missing data $\mathbf{P}''$. Note that the propagation operators $\hat{\mathbf{W}}_m$ are calculated from a background velocity model. For the inversion procedure, all the quantities to estimate are initially set to zero and then they are updated every iteration in such a way that the defined objective function decreases.

We choose our objective function J to be minimized as:

$$J = ||\mathbf{P} - \sum_{m=1}^{M} \hat{\mathbf{W}}_m^T \hat{\mathbf{R}}_m \hat{\mathbf{W}}_m \mathbf{Q}||^2, \qquad \mathbf{Q} = \mathbf{S} + R^{\cap}\mathbf{P}, \tag{4}$$

where M is again the number of focal regions, $\mathbf{Q}$ is the effective down-going wavefield at the surface, and $\mathbf{P} = \mathbf{P}' + \mathbf{P}''$ is our total data (measured + reconstructed, respectively). Then the update of $\hat{\mathbf{R}}_m^{\cup}$ (in each focal region) during the inversion can be written as:

$$\Delta\hat{\mathbf{R}}_m^{\cup} = -\hat{\mathbf{W}}_m^*(\mathbf{P} - \hat{\mathbf{W}}_m^T \hat{\mathbf{R}}_m \hat{\mathbf{W}}_m \mathbf{Q})\mathbf{Q}^H \hat{\mathbf{W}}_m^H. \tag{5}$$

Note in this expression the term $\mathbf{F}_m\{\cdot\} = \hat{\mathbf{W}}_m^*\{\cdot\}\hat{\mathbf{W}}_m^H$ actually is the definition of the bi-focal transform $\mathbf{F}$ related to a depth level m (Kutscha et al., 2010). Appliying the bi-focal transform to the seismic data is equivalent to taking all sources and receivers and virtually burry them into the subsurface at depth level z_m. In equation 5, $\Delta\hat{\mathbf{R}}_m^{\cup}$ is the bi-focal transform of $-(\mathbf{P} - \hat{\mathbf{W}}_m^T \hat{\mathbf{R}}_m \hat{\mathbf{W}}_m \mathbf{Q})\mathbf{Q}^H$ related to a particular focal boundary m: $\Delta\hat{\mathbf{R}}_m^{\cup} = -\mathbf{F}_m\{(\mathbf{P} - \hat{\mathbf{W}}_m^T \hat{\mathbf{R}}_m \hat{\mathbf{W}}_m \mathbf{Q})\mathbf{Q}^H\}$. In the first iteration $\Delta\hat{\mathbf{R}}_m^{\cup} = \mathbf{F}_m\{\mathbf{P}\mathbf{P}^H\}$, which describes the focusing of the data autocorrelation at depth level z_m.

Once $\Delta\hat{\mathbf{R}}_m^{\cup}$ is calculated for all focal regions, a sparsity condition is imposed on it by picking the strongest amplitudes in the reflectivity update (or focal domain) for each iteration, to produce a sparse update $\Delta\hat{\hat{\mathbf{R}}}_m^{\cup}$. This procedure will first explain the most predominant contributions to the reflectivity, while taking care of the small details in later iterations. Note that one single spike in the focal domain can explain an entire 3D response (primary + multiples) of a particular focal boundary, as can be seen from equation 2. This is very important as it means that we are physically accounting for the entire $\mathbf{X}_0$ response, just by applying a sparsity constraint on $\Delta\hat{\mathbf{R}}_m^{\cup}$ to get its spiky behavior. This process will allow us to interpolate big data gaps, as it will provide the full response of the associated focal region, even in locations where data was not measured.

Next, the reflectivity of every focal region can be updated by

$$\hat{\mathbf{R}}_{m,(i+1)}^{\cup} = \hat{\mathbf{R}}_{m,(i)}^{\cup} + \alpha\Delta\hat{\hat{\mathbf{R}}}_{m,(i)}^{\cup}, \tag{6}$$

where i is the iteration number and α is a suitable scaling constant such that J in equation 4 is minimized. Then the estimated impulse response $\hat{\mathbf{X}}_0$ of the current iteration can be calculated via eq. 3. After this step, inversion for constraining the source wavelet $S(\omega)$ and the missing data $\mathbf{P}''$ is performed as described in the orginal EPSI algorithm by van Groenestijn and Verschuur (2009a). These updates are given by

$$\Delta\mathbf{S} = -\hat{\mathbf{X}}_0^H(\mathbf{P} - \hat{\mathbf{X}}_0\mathbf{Q}), \qquad \Delta\mathbf{P}'' = -(\mathbf{I} + \hat{\mathbf{X}}_0)^H(\mathbf{P}' + \mathbf{P}'' - \hat{\mathbf{X}}_0\mathbf{Q}), \tag{7}$$

DOI http://dx.doi.org/10.1190/segam2013-1129.1

for the source wavelet and the missing data, respectively. These updates are then used for building up the entire estimation in an iterative approach with

$$\mathbf{S}_{(i+1)} = \mathbf{S}_{(i)} + \beta\Delta\mathbf{S}_{(i)}, \qquad \mathbf{P}''_{(i+1)} = \mathbf{P}''_{(i)} + \gamma\Delta\mathbf{P}''_{(i)}, \quad (8)$$

where the scaling constants β and γ are selected such that the objective function J is minimized. Finally, the entire primary estimation $\mathbf{P}_0$ (at all spatial locations) is then obtained via

$$\mathbf{P}_0 = \mathbf{X}_0\mathbf{S} \approx \sum_{m=1}^{M} \hat{\mathbf{W}}_m^T \hat{\mathbf{R}}_m^{\cup} \hat{\mathbf{W}}_m \hat{\mathbf{S}}. \quad (9)$$

EXAMPLE

In this section we will show one example of the proposed EPSI algorithm applied to synthetic 3D data. A constant velocity two-flat-layer model, with reflective boundaries located at 100 m and 300 m depth, and a grid of 20 shots and 20 receivers (in every direction) is used for the forward modeling. The offset range is kept limited to prevent the data volume from growing too much. An under-sampled acquisition is simulated by muting 3 out of 4 receiver lines in the seismic data. Then the proposed EPSI algorithm is used to reconstruct the missing data and to estimate the primary responses.

Figures 1 and 2 show the focal domains related to the primary responses after the inversion process. Primary information from each layer is mapped into sparse events localized around zero time. These sparse events contain the information necessary to explain the corresponding primary responses and their multiple reflections in 3D.Note that by 3 these events can be calculated for any source-receiver location, this allows reconstruction over large gaps.

Figures 3, 4 and 5 show the original coarse input data, the reconstructed input data and the primary estimation results of the described EPSI algorithm for one 3D shot record. These figures are composed by a set of 2D panels placed next to each other; each of these panels represents a 2D cross-section from the full 3D shot. As we can see from Figures 4 and 5, the described EPSI algorithm provides confident data reconstruction and a fully sampled estimated primary dataset. These results show the potential of the focal domain in data reconstruction allowing the extension of the original EPSI algorithm to 3D.

In this example the propagation operators from the surface to the focal boundaries, $\hat{\mathbf{W}}_1$ and $\hat{\mathbf{W}}_2$ are approximated using NMO velocities. However, for the focal domain parameterization the propagation operators don't have to be exact as long as they provide enough focusing of the data.

CONCLUSIONS

In this paper we have introduced a method to extend the current EPSI methodology such that it allows primary estimation on heavily under-sampled data. This can be useful for 2D data, but becomes mandatory for 3D data, were the data gaps tend to be much larger. The method described in this paper follows many of the same equations of the original EPSI method, but now a different parameterization is chosen: the effective generalized subsurface reflectivity $\hat{\mathbf{R}}_m$ is found via inversion, rather than the primary impulse response $\mathbf{X}_0$, as done in the original EPSI. To represent the data efficiently the focal domain $\mathbf{R}_m$ is described in terms of focal regions, and a sparsity constraint is imposed to the reflectivity update $\Delta\hat{\mathbf{R}}_m$.

The processing steps follow EPSI's full waveform inversion scheme in which the source wavelet $S(\omega)$, and the missing data $\mathbf{P}''$, are iteratively estimated together with $\mathbf{R}_m$ to produce the estimated primaries $\mathbf{P}_0$. Missing data is also reconstructed such that the final primary result is fully sampled. Illustrative examples show the capabilities of the proposed approach for a simple 3D example. Here, heavy under-sampling is overcome with data reconstruction. As an output we obtain fully sampled input data, fully sampled primaries, and the estimated source wavelet, based on a coarsely sampled input data and a crude background velocity model (used to calculate the approximate propagation operators).

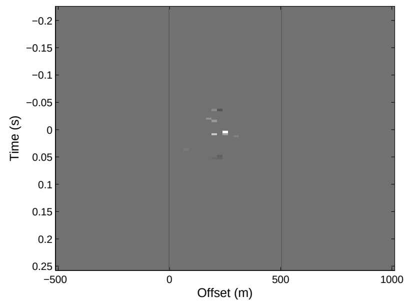

Figure 1: First focal region. The first primary is focused at zero time. Three central panels from a single 3D shot gather are shown.

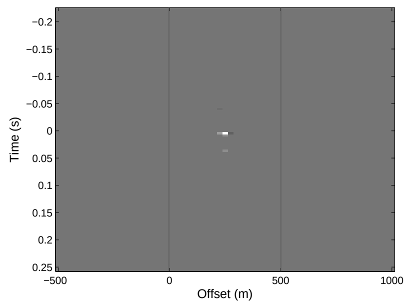

Figure 2: Second focal region. The second primary is focused at zero time. Three central panels from a single 3D shot gather are shown.

ACKNOWLEDGEMENTS

We thank the sponsors of the Delphi consortium for their support.

DOI http://dx.doi.org/10.1190/segam2013-1129.1

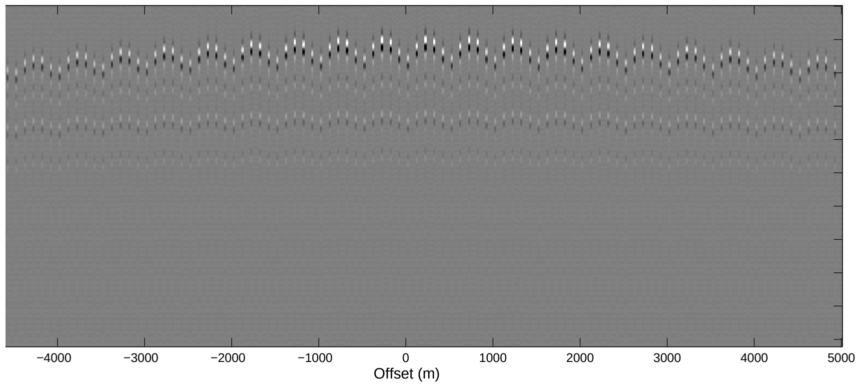

Figure 3: Selected shot record from a 3D data volume. 2D cross-section panels from the 3D gather are shown. Here 5 receiver positions were measured and 15 receiver positions in the crossline direction were missing for every shot.

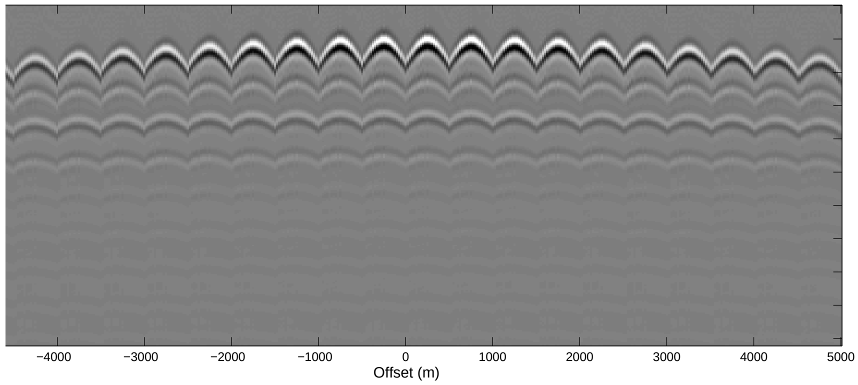

Figure 4: Reconstructed shot record from a 3D data volume. 2D cross-section panels from the full 3D data are shown. Here 5 receiver positions were measured and 15 receiver positions in the crossline direction were reconstructed for every shot.

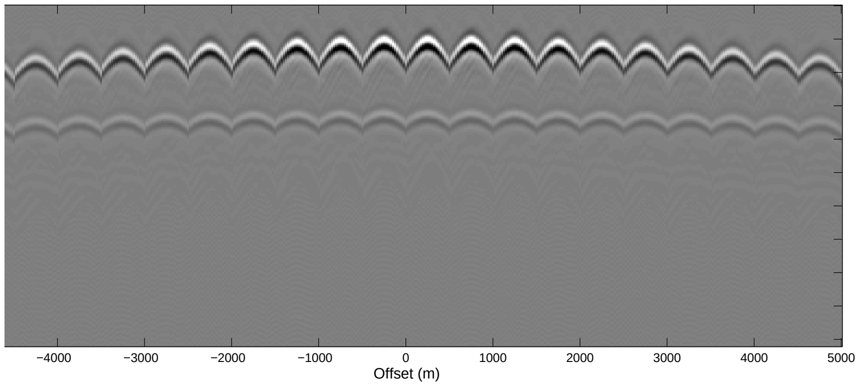

Figure 5: EPSI's primary estimation for the record shown in Figure 3. 2D cross-section panels from the full 3D results are shown. Primary information is now fully sampled, clearly revealing the primaries from this two-reflector model.

DOI http://dx.doi.org/10.1190/segam2013-1129.1

http://dx.doi.org/10.1190/segam2013-1129.1

EDITED REFERENCES

Note: This reference list is a copy-edited version of the reference list submitted by the author. Reference lists for the 2013 SEG Technical Program Expanded Abstracts have been copy edited so that references provided with the online metadata for each paper will achieve a high degree of linking to cited sources that appear on the Web.

REFERENCES

Aaron, P., R. O'Toole, S. Barnes, R. F. Hegge, and R. G. van Borselen, 2008, True-azimuth versus zero-azimuth 3D multiple prediction in WATS processing: 78th Annual International Meeting, SEG, Expanded Abstracts, Expanded Abstracts, 2431–2435.

Baardman, R. H., D. J. Verschuur, R. G. van Borselen, M. O. Frijlink, and R. F. Hegge, 2010, Estimation of primaries by sparse inversion using dual sensor data: 80th Annual International Meeting, SEG, Expanded Abstracts, Expanded Abstracts, 3468–3472.

Baumstein, A., M. T. Hadidi, D. L. Hinkley, and W. S. Ross, 2005, A practical procedure for application of 3D SRME to conventional marine data: The Leading Edge, **24**, 254–258.

Berkhout, A. J., 1982, Seismic migration, imaging of acoustic energy by wave field extrapolation, A: Theoretical aspects: Elsevier.

Berkhout, A. J., and D. J. Verschuur, 1997, Estimation of multiple scattering by iterative inversion, Part I: Theoretical considerations: Geophysics, **62**, 1586–1595.

Berkhout, A. J., and D. J. Verschuur, 2006, Focal transformation, an imaging concept for signal restoration and noise removal: Geophysics, **71**, no. 6, A55–A59.

Biersteker, J., 2001, Shell's surface multiple attenuation technique: 71st Annual International Meeting, SEG, Expanded Abstracts, Expanded Abstracts, 1301–1304.

de Briun, C. G. M., C. P. A. Wapenaar, and A. J. Berkhout, 1992, Angle-dependent reflectivity by means of prestack migration: Geophysics, **55**, 1223–1234.

Doulgeris, P., D. J. Verschuur, and G. Blacquiere, 2012, Separation of blended data by sparse inversion utilizing surface-related multiples: 74th Annual International Conference and Exhibition, EAGE, Extended Abstracts, 1–4.

Dragoset, W. H., I. Moore, and M. Yu, andW. Zhao, 2008, 3D general surface multiple prediction: An algorithm for all surveys: 78th Annual International Meeting, SEG, Expanded Abstracts, Expanded Abstracts, 2426–2430.

Dragoset, W. H., D. J. Verschuur, I. Moore, and R. Bisley, 2010, A perspective on 3D surface-related multiple elimination: Geophysics, **75**, no. 5, 75A245–75A261.

Kinneging, N. K., V. Budejicky, C. P. A. Wapenaar, and A. J. Berkhout, 1989, Efficient 2D and 3D shot record redatuming: Geophysical Prospecting, **37**, 493–530.

Kutscha, H., D. J. Verschuur, and A. J. Berkhout, 2010, High-resolution double focal transformation and its application to data reconstruction: 80th Annual International Meeting, SEG, Expanded Abstracts, Expanded Abstracts, 3589–3593.

Lin, D., J. Young, and Y. Huang, 2004, 3D SRME application in the Gulf of Mexico: 66th Annual International Conference and Exhibition, EAGE, Extended Abstracts, G035.

Lin, T. Y., and F. J. Herrmann, 2010, Sparsity-promoting migration from surface-related multiples: 80th Annual International Meeting, SEG, Expanded Abstracts, Expanded Abstracts, 3333–3337.

Moore, I., and R. Bisley, 2005, 3D surface-related multiple prediction (SMP): A case history: The Leading Edge, **24**, 270–284.

Savels, T., K. de Vos, and J. W. de Maag, 2011, Surface multiple attenuation through sparse inversion; results for complex synthetics and real data: First Break, **29**, 55–64.

Smith, P., B. Szydlik, and T. Traylen, 2011, True-azimuth 3D SRME in the Norwegian Sea: The Leading Edge, **30**, 928–931.

van Borselen, R. G., M. A. Schonewille, and R. F. Hegge, 2005, 3D surface-related multiple elimination: Acquisition and processing solutions: The Leading Edge, **24**, 260–268.

van Dedem, E. J., and D. J. Verschuur, 2005, 3D surface-related multiple prediction: A sparse inversion approach: Geophysics, **70**, no. 3, V31–V43.

van Groenestijn, G.J.A., and D. J. Verschuur, 2009a, Estimating primaries by sparse inversion and application to near-offset data reconstruction: Geophysics, **74**, no. 6, A23–A28.

van Groenestijn, G.J A., and D. J. Verschuur, 2009b, Estimation of primaries and near offsets by sparse inversion: Marine data applications: Geophysics, **74**, no. 6, R119–R128.

Verschuur, D. J., and A. J. Berkhout, 1997, Estimation of multiple scattering by iterative inversion, Part II: Practical aspects and examples: Geophysics, **62**, 1596–1611.

Verschuur, D. J., A. J. Berkhout, and C.P.A. Wapenaar, 1992, Adaptive surface-related multiple elimination: Geophysics, **57**, 1166–1177.

Weglein, A. B., F. A. Gasparotto, P. M. Carvalho, and R. H. Stolt, 1997, An inverse scattering series method for attenuating multiples in seismic reflection data: Geophysics, **62**, 1975–1989.

DOI http://dx.doi.org/10.1190/segam2013-1129.1